Low-Temperature Stabilization and Spectroscopic Characterization of the Dioxygen Complex of the Ferrous Neuronal Nitric Oxide Synthase Oxygenase Domain†

Amy P. Ledbetter,‡,§ Kirk McMillan,|| Linda J. Roman,⊥ Bettie Sue Siler Masters,⊥ John H. Dawson,*,‡,@ and Masanori Sono*,‡

Department of Chemistry and Biochemistry and School of Medicine, University of South Carolina, Columbia, South Carolina 29208, Department of Biochemistry, The University of Texas Health Science Center, San Antonio, Texas 78284-7760, and Pharmacopeia, Inc., Cranbury, New Jersey 08512

Received March 17, 1999

ABSTRACT: Nitric oxide (NO), an intercellular messenger and an immuno-cytotoxic agent, is synthesized by the family of nitric oxide synthases (NOS), which are thiolate-ligated, heme-containing monooxygenases that convert L-Arg to L-citrulline and NO in a tetrahydrobiopterin (BH_4)-dependent manner, using NADPH as the electron donor. The dioxygen complex of the ferrous enzyme has been proposed to be a key intermediate in the NOS catalytic cycle. In this study, we have generated a stable ferrous−O_2 complex of the oxygenase domain of rat neuronal NOS (nNOS) by bubbling O_2 through a solution of the dithionite-reduced enzyme at −30 °C in a cryogenic solvent containing 50% ethylene glycol. The most stable dioxygen complex is obtained using the oxygenase domain which has been preincubated for an extended length of time at 4 °C with BH_4/dithiothreitol and N^G-methyl-L-arginine, a substrate analogue inhibitor. The O_2 complex of the nNOS oxygenase domain thus prepared exhibits UV−visible absorption (maxima at 419 and 553 nm, shoulder at ∼585 nm) and magnetic circular dichroism spectra that are nearly identical to those of ferrous−O_2 cytochrome P450-CAM. Our spectral data are noticeably blue-shifted from those seen at 10 °C for a short-lived transient species (λ_{max} = 427 nm) for the nNOS oxygenase domain using stopped-flow rapid-scanning spectroscopy [Abu-Soud, H. M., Gachhui, R., Raushel, F. M., and Stuehr, D. J. (1997) *J. Biol. Chem. 272*, 17349], but somewhat similar to those of a relatively stable O_2 adduct of L-Arg-free full-length nNOS (λ_{max} = 415−416.5 nm) generated at −30 °C [Bec, N., Gorren, A. C. F., Voelder, C., Mayer, B., and Lange, R. (1998) *J. Biol. Chem. 273*, 13502]. Compared with ferrous−O_2 P450-CAM, however, the ferrous−O_2 adduct of the nNOS oxygenase domain is considerably more autoxidizable and the O_2−CO exchange reaction is noticeably slower. The generation of a stable ferrous−O_2 adduct of the nNOS oxygenase domain, as described herein, will facilitate further mechanistic and spectroscopic investigations of this important intermediate.

Nitric oxide (NO[1]), a signaling molecule and a cytotoxic agent, is synthesized by the family of heme-containing monooxygenase enzymes known as nitric oxide synthases (NOS). Three NOS isoforms consisting of the brain neuronal (nNOS), endothelial (eNOS), and macrophage (iNOS) enzymes exist (*1*−*6*). NOS is similar to cytochrome P450 in that both enzymes are cysteine thiolate-ligated heme proteins that share many spectral properties (*7*−*12*), but these two monooxygenases are distinctly different in their active site (heme pocket) and tertiary structures (*13*, *14*). Unlike P450, NOS requires tetrahydrobiopterin (BH_4) and bound calcium−calmodulin for activity. All NOS isoforms contain a C-terminal reductase domain that has the binding sites for FAD, FMN, and NADPH and an N-terminal oxygenase domain that has the binding sites for heme, BH_4, and the substrate L-Arg (*1*−*6*). Between the two domains of all three isoforms lies the binding site for calcium−calmodulin (*15*, *16*).

BH_4 plays a role in the stabilization of NOS in its catalytically active homodimer by binding in the dimer interface on the proximal side opposite of the substrate binding site of the heme (*13*, *50*). Bound BH_4 influences the heme spin state, substrate binding, and thermal stability of the protein (*13*, *17*−*20*). Questions remain as to whether BH_4 plays a redox role as it does in aromatic amino acid

† This work was supported by Grants GM-26730 (to J.H.D.) and HL-30050 and GM-52419 (to B.S.S.M.) from the U.S. Public Health Service and Grant AQ-1192 from The Robert A. Welch Foundation (to B.S.S.M.). This work was presented at the Fourth International Symposium on P450 Biodiversity and Biotechnology, Strasbourg, France, July 12−16, 1998.

* To whom correspondence should be addressed: Department of Chemistry and Biochemistry, University of South Carolina, Columbia, SC 29208. Phone: (803) 777-7234. Fax: (803) 777-9521. E-mail: msono@psc.sc.edu, dawson@psc.sc.edu.

‡ Department of Chemistry and Biochemistry, University of South Carolina.

§ To be submitted by A.P.L. in partial fulfillment of the Ph.D. requirements at the University of South Carolina.

|| Pharmacopeia, Inc.

⊥ The University of Texas Health Science Center.

@ School of Medicine, University of South Carolina.

[1] Abbreviations: NO, nitric oxide; NOS, nitric oxide synthase; nNOS, neuronal nitric oxide synthase; iNOS, macrophage inducible nitric oxide synthase; BH_4, tetrahydrobiopterin; BH_2, dihydrobiopterin; L-Arg, L-arginine; NOH-L-Arg, N^G-hydroxy-L-arginine; NMA, N^G-methyl-L-arginine; DTT, dithiothreitol; MCD, magnetic circular dichroism; P450, cytochrome P450; P450-CAM, camphor-metabolizing cytochrome P450 isolated from *Pseudomonas putida*; P420, denatured form(s) of cytochrome P450.

10.1021/bi990619h CCC: $18.00
Published on Web 06/03/1999

hydroxylases in which it is oxidized to the quinonoid BH_2 (*21*, *22*).

NOS converts L-Arg to L-citrulline and NO via two distinct oxidative steps (*5*, *23*). The first step in the catalysis of NOS is the formation of N^G-hydroxy-L-arginine (NOH-L-Arg) (see Scheme 1 in ref *24*) (*5*, *24*). On the basis of the similarity to P450 chemistry for N-hydroxylation (*25*−*27*), it has been proposed that the conversion of L-Arg to NOH-L-Arg requires reduction of the ferric heme, binding O_2 to form the ferrous−dioxygen adduct, and activating O_2 to form a high-valence electrophilic oxo−ferryl porphyrin π-cation radical species (equivalent to peroxidase compound I) (*1*, *5*, *24*). The compound I-type reactive oxygen species will then allow oxygen insertion into one of the two terminal guanidino nitrogens in L-Arg (*5*, *23*) by the so-called oxygen rebound mechanism (*25*, *27*−*29*). The second step of NOS catalysis converts NOH-L-Arg to L-citrulline and NO. Again, it has been proposed that this step requires the binding of dioxygen to the ferrous enzyme but, unlike the first step, does not involve the compound I-type species (*5*, *24*). Instead, the O_2 adduct is proposed to act as an oxidant by removing an electron (or hydrogen atom) from the *N*-hydroxy group of NOH-L-Arg to form the ferric peroxide intermediate and an $^{\bullet}$NO-L-Arg radical. The peroxo−iron species carries out a nucleophilic attack on the substrate guanidino carbon atom to form a heme iron-bound peroxy−substrate intermediate that breaks down to form L-citrulline and NO (*5*, *24*). The second step of the NOS reaction is similar to the proposed role of a ferric peroxide species in the last step of the P450−aromatase reaction (*25*, *27*).

Since the ferrous dioxygen complex of NOS is one of the key catalytic intermediates, it is important to isolate and spectroscopically characterize it. Recently, there has been a report showing the first evidence of O_2 binding to the heme iron of the nNOS oxygenase domain using rapid-scanning stopped-flow spectroscopy (*30*). The half-life ($t_{1/2}$) for autoxidation of this dioxygen species at 10 °C is 0.07 s in the presence of BH_4 (with or without L-Arg) and 4.9 s in the absence of BH_4 (with L-Arg) (*30*). In this study, we have been able to generate a much more stable dioxygen complex of the nNOS oxygenase domain at −30 °C ($t_{1/2} \sim 45$ min for autoxidation) in a cryogenic solvent and to demonstrate O_2−CO exchange using a sample that contains a substrate analogue inhibitor N^G-methyl-L-arginine (NMA) and BH_4. The spectral properties of our dioxygen nNOS complex are somewhat different from those reported previously (*30*), but closely resemble those (UV−visible absorption and MCD spectra) of the P450-CAM$^{\bullet}O_2$ complex (*31*).

Following completion of this study (see the title footnote), a paper by Lange, Mayer, and co-workers appeared which reports the reactions of calmodulin-free full-length nNOS as well as its oxygenase domain with dioxygen at −30 °C in 50% ethylene glycol (*32*). These researchers have reported formation of an O_2 complex ($t_{1/2} = 6.5$ min for autoxidation) only with the substrate (L-Arg)-free full-length nNOS in the presence and absence of tightly bound BH_4. Their nNOS intermediate has spectral properties that are somewhat similar ($\lambda_{max} = 415$−416.5 nm) to those reported herein ($\lambda_{max} = 419$ nm) for the nNOS oxygenase domain−O_2 complex. However, the lack of both further spectroscopic characterization of their complex and demonstration of O_2−CO exchange leaves some uncertainty regarding the firm identification of this species as oxyferrous nNOS.

MATERIALS AND METHODS

Materials. O_2 and CO gases were obtained from National Welders and Matheson Co., respectively. BH_4, NMA, and 7,8-BH_2 were purchased from Research Biochemicals International, Alexis Biochemicals, and Dr. B. Schirck's Laboratory (Jona, Switzerland), respectively. All other chemicals were purchased from Sigma or Aldrich and were used as received. The nNOS oxygenase domain (N-terminal amino acid residues 1−714) was prepared as described previously (*33*).

Preparation of Samples for MCD/UV−Visible Absorption Spectroscopy. The low-spin form of ferric nNOS oxygenase domain ($\epsilon_{419} = 100$ mM^{-1} cm^{-1}, this work)[2] was incubated at 4 °C in 50 mM potassium phosphate (pH 6.5) containing 10% glycerol in the presence of 0.5 mM NMA, 0.25 mM BH_4, and 2.5 mM DTT to convert the domain to a high-spin form. To 200 μL of the incubated sample was added 300 μL of ethylene glycol. The pH was then raised from 6.5 to 7.8 by careful addition of 1 M potassium hydroxide (7.5 μL). The pH values were monitored indirectly for the same buffer in the absence of nNOS and ethylene glycol. The sample was reduced at 4 °C under N_2 in a rubber septum-sealed cuvette by stepwise 10−15 μL microsyringe additions of an anaerobically prepared solution of sodium dithionite (50 mg in 50 mL of water). The reduction of the ferric enzyme to the deoxy−ferrous form was carefully monitored spectrophotometrically at 4 °C to avoid excessive addition of dithionite. The sample now containing ∼50% ethylene glycol was then cooled to −30 °C and gently bubbled with cold O_2 (less than or equal to −30 °C) for ∼30 s in a chest freezer box. The formation of the dioxygen complex of nNOS was monitored by MCD and UV−visible absorption spectroscopy at −30 °C. Concentrations of heme-containing enzyme were determined by the pyridine hemochromogen assay ($\epsilon_{556} = 34$ mM^{-1} cm^{-1}) (*34*).

UV−Visible Absorption and MCD Spectroscopy. UV−visible absorption spectra were obtained using Varian Cary 219 and 210 spectrophotometers. The MCD spectra were obtained using Jasco J-500A spectropolarimeter fitted with a Jasco MCD-1B electromagnet operated at 1.41 T as described in detail elsewhere (*35*). All spectral recordings were carried out at either 4 or −30 °C by circulating a 50% or 70% (v/v) methanol bath through the cell holder or by using a Barnes variable-temperature chamber. A 0.2 or 1 cm rubber septum-sealed cuvette was used.

RESULTS AND DISCUSSION

Optimal Sample Conditions for Generation of a Stable Ferrous Dioxygen Complex of the nNOS Oxygenase Domain. To develop the optimum sample for stabilizing the ferrous−dioxygen nNOS adduct, several conditions were examined. Initially, the low-spin ferric nNOS oxygenase domain in the absence of L-Arg and BH_4 (spectrum a, Figure 1A) was reduced with dithionite in a mixed solvent [50% ethylene glycol and 20 mM phosphate or Tris [tris(hydroxymethyl)-

[2] M. Sono, A. P. Ledbetter, K. McMillan, L. J. Roman, B. S. S. Masters, and J. H. Dawson, submitted for publication.

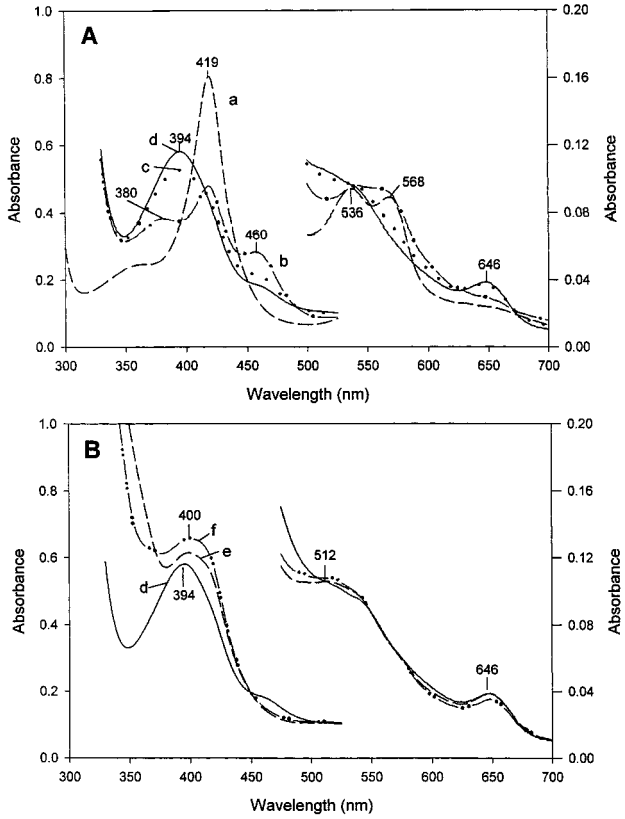

FIGURE 1: UV−visible absorption spectral changes of the nNOS oxygenase domain from low-spin to high-spin upon addition of 0.5 mM NMA and 0.25 mM BH_4/2.5 mM DTT as a function of incubation time. Concomitant addition of NMA (0.5 mM) and BH_4 (0.25 mM) together with DTT (2.5 mM) at pH 6.5 quickly (<30 s) converted the low-spin-type absorption spectrum of the oxygenase domain (spectrum a) (originally 16 μM) to that of a partially DTT-bound derivative (spectrum b). After incubation for 17 h at 4 °C, the spectrum changed to that of a high-spin type (spectrum c). Further incubation for a total of 69 h resulted in spectrum d. Additional incubation gave spectrum e (total of 7 days) and spectrum f (total of 3.5 months). A 0.5 cm cuvette was used.

aminomethane hydrochloride]] at 4 °C and pH 7.4 or 8.5 and bubbled with O_2 at −30 °C. Unfortunately, at either pH, the reduced nNOS oxygenase domain did not form a detectable O_2 complex but instead readily autoxidized back to the ferric low-spin state. A separate sample of the domain was then incubated in the dark (because of the photosensitivity of BH_4) at 4 °C with 0.5 mM NMA (a substrate analogue inhibitor), 0.25 mM BH_4, and 2.5 mM DTT, which was used to maintain BH_4 in its reduced form (*36*). The absorption spectrum of the protein changed initially to that of a partially DTT-bound species (λ_{max} = 380 and 460 nm) (spectrum b, Figure 1A). Over time, the sample underwent a low-spin (six-coordinate) to high-spin (five-coordinate)-type spectral change exhibiting new Soret and visible bands at 394 and 646 nm, respectively (spectra c and d, Figure 1). This spectral change does not occur in the absence of BH_4 and DTT and is most likely due to binding of BH_4 and NMA to the active site of the nNOS oxygenase domain.[2] Attempts to generate a stable dioxygen complex were unsuccessful with sample d in Figure 1. Samples prepared under conditions (incubation for 7 days) similar to those for sample e did form a spectrally detectable dioxygen complex but with a somewhat poor stability ($t_{1/2}$ ∼ 6 min) (vide infra). Fortunately, the conditions used to prepare sample f, including incubation with NMA, BH_4, and

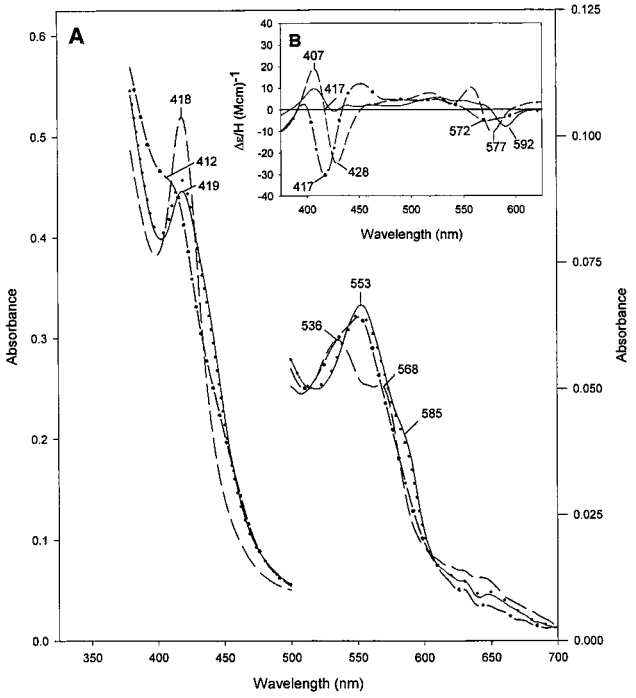

FIGURE 2: (A) UV−visible absorption and (B) MCD spectra of the nNOS oxygenase domain prepared from sample f in Figure 1B in 50% (v/v) ethylene glycol and 17.5 mM potassium phosphate (pH 7.8) containing 0.087 mM biopterin, 0.87 mM DTT/oxidized DTT, and 0.17 mM NMA recorded at −30 °C in a 1 cm cuvette. Reduction of ferric nNOS (- − -) with dithionite results in ferrous nNOS (− · −). The ferrous nNOS was bubbled with oxygen to form the oxy-adduct nNOS (—). The spectrum shown in the dotted line was recorded after the dioxygen adduct stood for 11 min. The large absorbance below 400 nm is due to BH_2 species, the autoxidation products of BH_4 (*37*). The final protein (heme) concentration was 5.0 μM.

DTT at 4 °C for an extended length of time, gave satisfactory results as will be described below.

Spectral Monitoring of the Formation of the Dioxygen Complex. The UV−visible absorption spectrum of the nNOS sample which had been incubated for 3.5 months in the presence of BH_4/DTT and NMA (spectrum f, Figure 1B) is a predominantly high-spin type (λ_{max} = 400, 512, and ∼650 nm). The large absorbance below 400 nm is due to BH_2, an autoxidation product(s) of BH_4 formed following the depletion of DTT (see below). The integrity of the protein even after such a long incubation time was judged to be satisfactory by the lack of conversion to a P420 type (λ_{max} ∼ 420 nm) species upon dithionite reduction in the presence of CO using an aliquot of the sample.[3] When 1.5 volumes of ethylene glycol was added to the sample, its spectrum changed to a nearly complete low-spin type (Figure 2A, dashed line). The pH of the sample was raised to pH 7.8. The MCD spectrum of the ferric sample thus prepared in the mixed solvent exhibits a derivative-shaped feature centered at 417 nm and a trough at 577 nm (Figure 2B, dashed line), which is very similar to that of L-Arg- and BH_4-free low-spin nNOS oxygenase domain.[2] Once the sample is reduced with dithionite, the resulting ferrous derivative

[3] Under these incubation conditions, the ferric nNOS oxygenase domain became extremely stable. In contrast, incubation at 4 °C or even storage at −20 °C of the enzyme alone for such a long time led to significant formation of a P420-type ferrous−CO species.

absorbs at ∼412 nm and exhibits a single peak in the visible region at 553 nm (Figure 2A, dotted−dashed line). The MCD spectrum of the ferrous enzyme features a moderately intense trough in the Soret region at 417 nm and a relatively broad and less intense trough around 572 nm. These MCD spectral features are typical of five-coordinate high-spin ferrous nNOS (*12*).

After gentle bubbling with O_2 through the ferrous sample at −30 °C for ∼30 s, a new species appeared which absorbs at 419, 553, and ∼585 nm (shoulder) (Figure 2A, solid line). This enzyme species was stable enough to permit spectroscopic examinations to be performed. Over a period of 11 min, only a small spectral change (autoxidation, see below) occurred (from solid line to dotted line, Figure 2A) which corresponds to 13−15% of the total spectral conversion to fully oxidized enzyme (dashed line, Figure 2A). Although the reaction of dithionite (λ_{max} = 315 nm) with O_2 at −30 °C was much slower than that at ambient temperature, complete disappearance of dithionite in the nNOS oxygenase domain sample under these conditions was confirmed indirectly with a control experiment using a P450-CAM sample for which A_{315} was easily monitored. The MCD spectrum of the new species of the nNOS oxygenase domain recorded in 5 min following O_2 bubbling has a prominent peak at 407 nm and a trough at 592 nm (Figure 2B, inset, solid line). Since the ferric enzyme has a distinct MCD trough at 577 nm as described above, the new species was judged to be essentially homogeneous, i.e., free from the autoxidized species. To verify that the new species of the nNOS oxygenase domain thus generated at −30 °C is the ferrous−dioxygen complex, we have examined its CO exchange reaction and autoxidation.

CO Exchange and Autoxidation of the Dioxygen Complex. As shown in Figure 3A, after ferric nNOS (a) had been reduced with dithionite, bubbled with O_2 (b), and allowed to stand for ∼15 min at −30 °C, CO was gently bubbled into the sample for ∼15 s and the inside of the septum-sealed cuvette was filled with additional CO gas. Since spectral changes following CO bubbling were relatively small and quite slow, the CO-bubbled sample was warmed to ∼4 °C by immersing the cuvette in the circulator solvent for 30 s and then cooled to −30 °C by putting the cuvette back to the precooled cuvette holder, and its spectrum was recorded (spectrum c). Spectrum c was nearly identical to the spectrum of the starting ferric sample (a) except for the presence of a shoulder between 430 and 460 nm. The sample was again warmed to 4 °C and re-reduced with small grains of dithionite and bubbled with CO (spectrum d). These oxidation−reduction and ligand (O_2 and CO) binding−exchange reaction processes are schematically shown in Scheme 1, where the heme iron is shown as Fe^{3+} and Fe^{2+} and the letters a−d identify the samples whose spectra are displayed in Figure 3A.

Close examination of these spectral changes using difference spectra (vs ferric nNOS, spectrum a indicated that the shoulder in spectrum c can be attributed to a small fraction ($^1/_7 \sim 15\%$) of the ferrous−CO complex present in the predominantly (∼85%) ferric species formed via autoxidation. This is shown in Figure 3B where difference spectrum c′ (λ_{max} = 444.5 nm) is similar to that of the fully formed ferrous−CO adduct, spectrum d′ (λ_{max} = 445.5 nm), except for their intensities ($\Delta A_{445.5}$ for d′ ∼ $7\Delta A_{444.5}$ for c′).

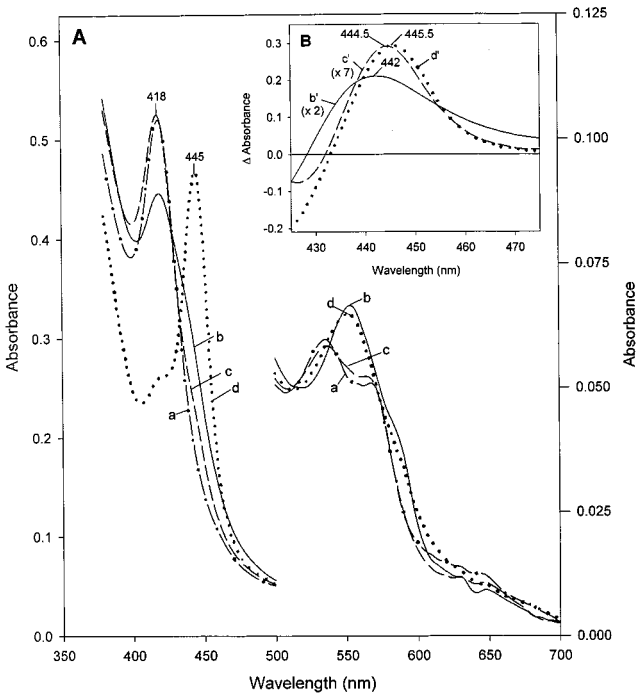

FIGURE 3: (A) Absolute UV−visible absorption and (B) difference spectra (vs the ferric spectrum) of the nNOS oxygenase domain after bubbling with O_2 and then CO at −30 °C. (A) Ferric domain (a), the ferrous−oxy complex (b), a mixture of ferric and ferrous−CO species formed after CO bubbling at −30 °C, warming up to 4 °C, and then cooling to −30 °C (c), and the ferrous−CO complex generated by further CO bubbling and dithionite addition at 4 °C (d). (B) Difference spectra, b′ (b − a), c′ (c − a), and d′ (d − a). Spectra b′ and c′ are enlarged 2 and 7 times, respectively.

Scheme 1

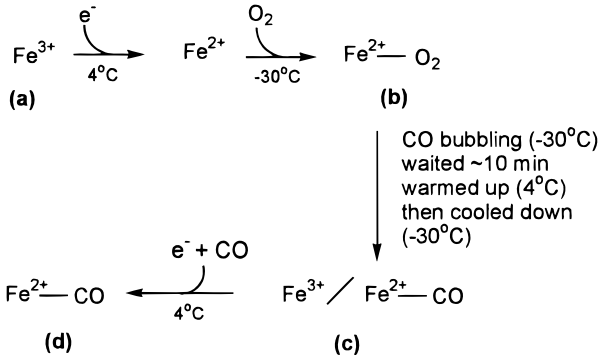

Difference spectrum c′ is clearly different from that of the ferrous−O_2 complex, spectrum b′ (λ_{max} = 442 nm).[4]

In separate experiments, the dioxygen complex of the nNOS oxygenase domain was observed to autoxidize to the low-spin ferric form. The reaction was followed by UV−visible absorption spectroscopy and displayed a single set of isosbestic points (429, 515, and 539 nm) (spectra not shown). This indicates that no detectable intermediates are involved in the autoxidation process. The autoxidation reaction at −30 °C was first-order with a rate constant of 1.5×10^{-2} min^{-1} ($t_{1/2}$ = 46 min) for the most stable dioxygen

[4] In the case of P450-CAM, the difference spectrum for the ferrous−CO minus low-spin ferric form (λ_{max} = 446 nm) can be similarly distinguished from that for the ferrous−O_2 minus low-spin ferric form (λ_{max} = 440 nm), where ΔA_{446} (ferrous−CO) = $\sim 4\Delta A_{440}$ (ferrous−O_2), as calculated in this study using previously published spectral data (*38*).

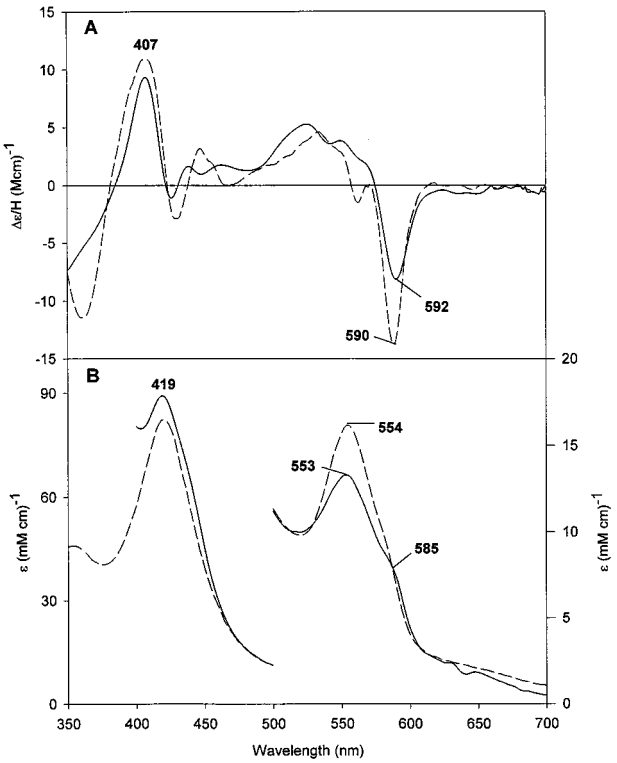

FIGURE 4: (A) MCD and (B) UV−visible spectra of the O_2 complex of nNOS and P450-CAM. The spectra of the P450-CAM·O_2 complex (- - -) (taken from ref *31*) and those of the oxy-nNOS oxygenase domain (—) (this work) were recorded at −30 °C in 50% ethylene glycol. The spectrum for the nNOS domain below 400 nm in panel B is omitted because of the large absorbance of BH_2 (*37*).

complex obtained in this work (shown in Figure 2). A regenerated dioxygen complex using the autoxidized oxy-nNOS oxygenase domain sample was less stable ($t_{1/2} \sim 6$ min) than the initial complex.

The results described above and summarized in Scheme 1 indicate that the binding of dioxygen to ferrous nNOS oxygenase domain is reversible. In other words, exchange of the bound O_2 for CO *does occur* even though the rate of CO exchange was extremely slow at −30 °C and can only be detected at higher temperatures. However, under the conditions employed in this study, autoxidation of the dioxygen complex is considerably faster (by more than 5 times, i.e., $^{85}/_{15}$) than the CO exchange reaction, leading to spectrum c in Figure 3.

Similarities and Differences between the Dioxygen Complexes of the nNOS Oxygenase Domain and P450-CAM. Both the MCD and UV−visible absorption spectra of the dioxygen complexes of the nNOS oxygenase domain and P450-CAM, overplotted in panels A and B of Figure 4, respectively, are very similar to each other throughout the spectral region that was examined. Both complexes have absorption bands (419 and ∼554 nm and a shoulder at ∼585 nm) and major Soret region MCD peaks (407 nm) and visible region troughs (∼590 nm) at almost the same positions. In a more detailed comparison, the UV−visible spectral feature in the visible region of nNOS is less intense than P450-CAM·O_2, but the shoulder at ∼585 nm is more pronounced for nNOS. Nevertheless, these close spectral similarities between the dioxygen complexes of nNOS and P450-CAM provide strong evidence of formation of the ferrous O_2 complex of nNOS. However, the reason for the somewhat different absorption band position for the transient O_2 complex ($\lambda_{max} = 427$ nm) observed by Stuehr and co-workers (*30*) as compared with that of our stabilized O_2 complex ($\lambda_{max} = 419$ nm) is not clear since both sets of data have been obtained using essentially identical nNOS oxygenase domain constructs.

On the other hand, the rates of the O_2−CO exchange reaction and autoxidation of the dioxygen complex of the nNOS oxygenase domain are markedly different from those of the P450-CAM·O_2 complex. For the P450-CAM·O_2 complex, O_2−CO exchange readily occurs even at −30 °C, as examined in this work as a control. The rate of O_2−CO exchange is expected to reflect a combined effect of the rates of O_2 dissociation from the complex and subsequent CO binding to the ferrous deoxy enzymes. At 23 °C, the ferrous deoxy form of the nNOS oxygenase domain in the presence of L-Arg and BH_4 binds CO at a rate (2.1×10^4 M^{-1} s^{-1} for a predominant slow phase; *39*) which is not significantly different from the rate (3.7×10^4 M^{-1} s^{-1}) for camphor-bound P450-CAM (*40*). The rate constant for O_2 dissociation from oxyferrous P450-CAM ($k_d = 25$ s^{-1}, temperature not specified) has been reported (*41*). The value for this reaction reported by Stuehr and co-workers ($k_d = 108$ s^{-1} at 10 °C) for the "ferrous−O_2" nNOS oxygenase domain (*30*) needs to be re-evaluated in light of the spectral differences between their oxyferrous adduct and the one described herein.

Autoxidation is much slower for the O_2 complex of camphor-bound P450-CAM ($t_{1/2} = 95$ min at pH 7.4 and −10 °C; *31*) than that for the nNOS oxygenase domain ($t_{1/2} \sim 45$ min at pH 7.8 and −30 °C; this study). In cryogenic mixed solvents (50% ethylene glycol), camphor-bound and camphor-free ferric P450-CAM are high- and low-spin, respectively (*42*), as they are in aqueous solution. It has been shown that the ferrous P450-CAM·O_2 complex is considerably more autoxidizable in the absence of the substrate camphor than in its presence (*42*). Interestingly, at −30 °C, the stabilities of the dioxygen complexes of the nNOS oxygenase domain ($t_{1/2} \sim 45$ min; this work) and camphor-free P450-CAM ($t_{1/2} = 155$ min; *42*) are somewhat similar even though the former is still less stable than the latter.

Roles of BH_4, DTT, and L-Arg (or NMA) in the Formation of the Stable Dioxygen Complex of the nNOS Oxygenase Domain. Without preincubation of the ferric domain with BH_4/DTT and substrate (or its analogue inhibitors), the dithionite-reduced nNOS oxygenase domain did not form a detectable dioxygen complex at −30 °C when examined in this study. This is in agreement with the results reported by Lange, Mayer, and co-workers (*32*). These researchers observed direct transition from the dithionite-reduced nNOS oxygenase domain to oxidized enzyme upon O_2 bubbling at −30 °C in the absence or presence of BH_4 and/or L-Arg. However, we have found in this study that only the nNOS oxygenase domain which had been incubated with BH_4/DTT and NMA (or L-Arg) for an extended length of time (spectrum f in Figure 1B) forms the most stable dioxygen complex.

The apparent effect of the incubation of the ferric nNOS oxygenase domain with BH_4 and L-Arg (or its analogues) is its conversion from a nearly complete low-spin (six-coordinate) to largely high-spin (five-coordinate) state (spectra a → → c → d in Figure 1A) via the partially (∼60%) DTT-bound low-spin state (b). Note that the heme-bound

DTT is mostly dissociated from the domain at the end of this process. This spectral change requires the concomitant presence of BH_4, DTT, and L-Arg (or NMA); each of these compounds alone or BH_4 with L-Arg does not cause such a spectral change even after incubation for 48 h. A combination of BH_4 and DTT (in the absence of L-Arg or NMA) has only a partial effect (conversion to ~70% high-spin in 48 h at pH 6.8 and 4 °C).[2] The failure of BH_4 and L-Arg (without DTT under aerobic conditions) to induce such spectral and spin state changes could be attributed to the fact that BH_4 is readily autoxidizable in aerobic solution and is converted to 7,8-BH_2 via the quinonoid form of BH_2 (*37*). DTT quickly reduces the quinonoid form of BH_2 back to BH_4 (*37*). However, additional experiments in this study have revealed several intriguing points concerning the roles of BH_4 and DTT in the low-spin to high-spin conversion of the ferric nNOS oxygenase domain as will be reported elsewhere in detail.[2] These findings are summarized as follows. (a) 7,8-BH_2 is as effective as BH_4 for this spin conversion when used in combination with DTT and L-Arg (or NMA). This observation is consistent with the results recently reported by Stuehr and co-workers using an iNOS oxygenase domain (*43*). Somewhat unexpectedly, (b) in the absence of DTT (or other thiols such as β-mercaptoethanol and cysteine),[2] a combination of BH_4 and L-Arg is incapable of converting the spin state of the nNOS oxygenase domain *even under anaerobic conditions* where autoxidation of BH_4 is prevented. On the other hand, (c) L-Arg and/or BH_4 (or BH_2) can shift the heme spin state only in the presence of DTT (or other thiols). Thus, DTT appears to play a critical role(s) in this process other than keeping BH_4 in its reduced form.

The BH_4-free low-spin nNOS oxygenase domain used in this study was judged to be dimeric on the basis of a gel-sizing column chromatogram (using Hiloard 26/60 Superdex 200 gel from Phrmacia) at a final step of its purification. Now, the following questions arise: (a) Why is the L-Arg/BH_4/DTT-induced spin state conversion (i.e., the binding of L-Arg and BH_4 to the oxygenase domain) required for the formation of a stable dioxygen complex of the domain? (b) Why is such a long incubation time (3.5 months) needed to form the most stable dioxygen complex even though the spin state change of the ferric oxygenase domain was achieved to ~80% completion in a much shorter (~24 h) incubation time (see Figure 1)? These questions are addressed below.

Upon closer spectral inspection of the sample components, it was determined that sample f (Figure 1B) contains a chemically nonreducible (even by dithionite) form of BH_2 (7,8-dihydrobiopterin) (*37*). In fact, under the aerobic conditions used (with 0.25 mM BH_4 and 2.5 mM DTT at pH 6.5 and 4 °C), half of BH_4 and all of BH_4 in the sample solution were converted to 7,8-BH_2 in about 4 and 7 days, respectively (this work). This is because DTT was gradually oxidized and totally depleted in about 1 week under these conditions. This BH_4 oxidation product (7,8-BH_2) only absorbs below 375 nm (*37*), as seen in spectrum f (Figure 1B) ($\lambda_{max} = 279$ and 328 nm at pH 6.8; this study, spectrum not shown). Neither DTT nor its oxidized species absorbs significantly above 260 or 350 nm, respectively (*44*). The inability of sample d (which still contains some BH_4 after incubation for ~3 days) to form a stable dioxygen complex is presumably due to the destabilizing influence of BH_4 ($\lambda_{max} \sim 300$ nm) (*37*, *45*) as proposed by Stuehr and co-workers (*30*). Free BH_4 in solution might be also contributing as a reductant to the accelerated autoxidation.

On the other hand, the ability of sample f to generate a stable dioxygen complex suggests that BH_2 does not accelerate autoxidation because it is not chemically reducible (*36*). In support of this speculation, a ferric nNOS oxygenase domain sample which had been completely converted to a high-spin state (spectrum similar to spectrum e in Figure 1) by incubation with BH_2/L-Arg (or NMA)/DTT at pH 6.5−7.5 and 4 °C for ~15 days was also shown in this study to form a spectrally detectable dioxygen complex at −30 °C (spectrum not shown, but similar to the solid line in Figure 2A). Although the oxy-nNOS domain thus generated was somewhat less stable ($t_{1/2} \sim 6$ min at pH 7.5 and −30 °C), the incubation time (~15 days) was considerably shorter than that (3.5 months) for the nNOS domain which had been incubated initially with BH_4/NMA/DTT and was used to generate the ferrous−O_2 adduct shown in Figures 2−4 (solid line). When a sample having an absorption spectrum similar to the solid line (d) in Figure 1, including a small absorption band at ~460 nm (the remaining DTT complex), was examined after an even shorter incubation time (for ~3 days) with BH_2/L-Arg (or NMA)/DTT, formation of the dioxygen complex was not observed. Thus, it appears that nearly complete conversion to a high-spin species of the ferric domain as judged by the loss of the shoulder at 460 nm is critical prior to addition of ethylene glycol (~50%) for the successful generation of the stable ferrous−O_2 complex. Since the substrate/pterin/DTT-induced slow spin state conversion of the ferric nNOS oxygenase domain occurs when the protein is already dimeric, such a spin state change most likely reflects a protein conformational change(s) within the dimer in the vicinity of the heme-bound active site which is necessary for formation of a stable dioxygen complex. Details of such a protein conformational change and the reason it requires such an extended incubation time are not entirely clear.

NMA is known to be a slow substrate as well as a mechanism-based inhibitor for NOS (*46*, *47*). NMA and L-Arg behave in a very similar manner in terms of binding affinity for ferric nNOS (*46*).[2] The UV−visible absorption spectral properties of the resulting complexes are also similar,[2] although subtle differences have been observed with EPR spectroscopy for their ferric (*48*) or ferrous−NO (*49*) complexes. Since oxygenated NOS is not expected to react with L-Arg in the first step of the NOS catalytic cycle (L-Arg → NOH-L-Arg), the stability and spectral properties of the dioxygen complex in the presence of NMA reported herein are likely to be similar when L-Arg is substituted for NMA. In this respect, the ferrous−O_2 nNOS oxygenase complex characterized in this study represents more closely the oxy-NOS intermediate species formed in the first step of the catalytic reaction than that in the second step. However, the intrinsic spectral properties (i.e., electronic structures) of the two oxy-NOS complexes formed in the two steps are expected to be similar. Further investigations are in progress focusing on the reactivities and additional spectroscopic properties of the dioxygen complexes of NOS under various conditions as well as on the postulated roles of several compounds used in stabilizing the dioxygen adduct of the enzyme.

Identification of the Dioxygen Complex of nNOS. Upon mixing O_2 with the dithionite-reduced enzyme, Lange, Mayer, and co-workers were able to detect a relatively slowly decaying ($t_{1/2}$ = 6.5 min for autoxidation) intermediate of substrate (L-Arg)-free full-length nNOS both in the presence and in the absence of tightly bound (in the molar ratio of 0.5 per heme) BH_4 (*32*). Note that the BH_4-bound nNOS sample contained less than stoichiometric amounts of BH_4 and no added free BH_4 in solution. The UV−visible absorption spectral properties of the intermediate (λ_{max} = 415−416.5 nm) are somewhat similar to those of the dioxygen complex of the nNOS oxygenase domain described herein (λ_{max} = 419 nm). The formation of the proposed, relatively stable dioxygen complex of full-length nNOS even in the absence of BH_4 can be attributed to the fact that the BH_4-free nNOS sample used was in a dimeric form (*18*) and likely had the proper active site structure. In the presence of L-Arg for intact nNOS which contained tightly bound BH_4, however, they observed another intermediate species whose absorption spectrum (λ_{max} = 404.5 nm) is decidedly different from the dioxygen complexes of any P450 isoforms. They propose that this species is BH_4-reduced ferrous−O_2 nNOS which is equivalent to the ferric−peroxide species. With the nNOS oxygenase domain, however, these researchers were unable to observe the oxygenated enzyme intermediate as already described above.

In view of the varying spectral properties and stabilities of the dioxygen-bound nNOS intermediate observed by three different groups (refs *30* and *32* and this paper), it is important to characterize the oxyferrous NOS species as thoroughly as possible. Given the powerful fingerprinting capability of MCD spectroscopy (*12*, *38*), this study involving close spectral comparison to the more fully characterized dioxygen adduct of P450-CAM (*38*) and the demonstration of CO exchange provides more conclusive identification of the intermediate as oxyferrous nNOS. Finally, the ability to prepare a stable dioxygen adduct of the nNOS oxygenase domain, a form of the enzyme lacking the flavin electron donor, opens up the possibility of further mechanistic studies.

ACKNOWLEDGMENT

We thank Dr. Alycen E. Pond for valuable discussions and for providing the O_2−CO exchange control experiments with P450-CAM and Drs. Edmund W. Svastits and John J. Rux for developing the computer-based spectroscopic data-handling system. The excellent technical assistance of Mr. Tom Shea (The University of Texas Health Science Center) in preparing the nNOS oxygenase domain is also gratefully acknowledged. In addition, we thank Dr. John W. Ledbetter (Medical University of South Carolina, Charleston, SC) for his generous gifts of 7,8-BH_2 and the Barnes Variable Temperature Chamber for allowing additional low-temperature experiments, and Chance Carter for his assistance in connecting the chamber to the Cary 210 spectrophotometer.

REFERENCES

1. Feldman, P. L., Griffith, O. W., and Stuehr, D. J. (1993) *Chem. Eng. News 71* (51), 26−38.
2. . Masters, B. S. S., McMillan, K., Sheta, E. A., Nishimura, J. S., Roman, L. J., and Martásek, P. (1996) *FASEB J. 10*, 552−558.
3. Nathan, C. (1992) *FASEB J. 6*, 3051−3064.
4. Stuehr, D. J., and Griffith, O. W. (1992) *Adv. Enzymol. Relat. Areas Mol. Biol. 65*, 287−346.
5. Marletta, M. A. (1993) *J. Biol. Chem. 268*, 12231−12234.
6. Bredt, D. S., and Snyder, S. H. (1994) *Annu. Rev. Biochem. 63*, 175−195.
7. White, K. A., and Marletta, M. A. (1992) *Biochemistry 31*, 6627−6631.
8. Stuehr, D. J., and Ikeda-Saito, M. (1992) *J. Biol. Chem. 267*, 20547−20550.
9. McMillan, K., Bredt, D. S., Hirsch, D. J., Snyder, S. H., Clark, J. E., and Masters, B. S. S. (1992) *Proc. Natl. Acad. Sci. U.S.A. 89*, 11141−11145.
10. Wang, J., Stuehr, D. J., Ikeda-Saito, M., and Rousseau, D. L. (1993) *J. Biol. Chem. 268*, 22255−22258.
11. Wang, J., Rousseau, D. L., Abu-Soud, H. M., and Stuehr, D. J. (1994) *Proc. Natl. Acad. Sci. U.S.A. 91*, 10512−10516.
12. Sono, M., Stuehr, D. J., Ikeda-Saito, M., and Dawson, J. H. (1995) *J. Biol. Chem. 270*, 19943−19948.
13. Crane, B. R., Arvai, A. S., Ghosh, D. K., Wu, E., Getzoff, E. D., Stuehr, D. J., and Tainer, J. A. (1998) *Science 279*, 2121−2126.
14. Poulos, T. L., Finzel, B. C., and Howard, A. J. (1987) *J. Mol. Biol. 195*, 687−700.
15. Bredt, D. S., Hwang, P. M., Glatt, C. E., Lowenstein, C., Reed, R. R., and Snyder, S. H. (1991) *Nature 351*, 714−718.
16. Abu-Soud, H. M., and Stuehr, D. J. (1993) *Proc. Natl. Acad. Sci. U.S.A. 90*, 10769−10772.
17. Presta, A., Siddhanta, U., Wu, C., Sennequier, N., Huang, L., Abu-Soud, H. M., Erzurum, S., and Stuehr, D. J. (1998) *Biochemistry 37*, 298−310.
18. Gorren, A. C., List, B. M., Schrammel, A., Pitters, E., Hemmens, B., Werner, E. R., Schmidt, K., and Mayer, B. (1996) *Biochemistry 35*, 16735−16745.
19. Salerno, J. C., Martásek, P., Roman, L. J., and Masters, B. S. S. (1996) *Biochemistry 35*, 7626−7630.
20. Salerno, J. C., Martásek, P., Williams, R. F., and Masters, B. S. S. (1997) *Biochemistry 36*, 11821−11827.
21. Kaufman, S. (1993) *Adv. Enzymol. Relat. Areas Mol. Biol. 67*, 77−264.
22. Dix, T., and Benkovic, S. J. (1988) *Acc. Chem. Res. 21*, 101−107.
23. Stuehr, D. J., Kwon, N. S., Nathan, C. F., Griffith, O. W., Feldman, P. L., and Wiseman, J. (1991) *J. Biol. Chem. 266*, 6259−6263.
24. Griffith, O. W., and Stuehr, D. J. (1995) *Annu. Rev. Physiol. 57*, 707−736.
25. Ortiz de Montellano, P. R. (1995) in *Cytochrome P-450: Structure, Mechanism, and Biochemistry* (Ortiz de Montellano, P. R., Ed.) 2nd ed., pp 245−303, Plenum Press, New York.
26. Guengerich, F. P., and Macdonald, T. L. (1990) *FASEB J. 4*, 2453−2459.
27. Sono, M., Roach, M. P., Coulter, E. D., and Dawson, J. H. (1996) *Chem. Rev. 96*, 2841−2887.
28. Mueller, E. J., Loida, P. J., and Sligar, S. G. (1995) in *Cytochrome P-450: Structure, Mechanism, and Biochemistry* (Ortiz de Montellano, P. R., Ed.) 2nd ed., pp 183−214, Plenum Press, New York.
29. Groves, J. T., McClusky, G. A., White, R. E., and Coon, M. J. (1978) *Biochem. Biophys. Res. Commun. 81*, 154−160.
30. Abu-Soud, H. M., Gachhui, R., Raushel, F., and Stuehr, D. J. (1997) *J. Biol. Chem. 272*, 17349−17353.
31. Sono, M., Eble, K. S., Dawson, J. H., and Hager, L. P. (1985) *J. Biol. Chem. 260*, 15530−15535.
32. Bec, N., Gorren, A. C. F., Voelder, C., Mayer, B., and Lange, R. (1998) *J. Biol. Chem. 273*, 13502−13508.
33. McMillan, K., and Masters, B. S. S. (1993) *Biochemistry 32*, 9875−9880.
34. Paul, K. G., Theorell, H., and Akeson, A. (1953) *Acta Chem. Scand. 7*, 1284−1287.
35. Huff, A. M., Chang, C. K., Cooper, D. K., Smith, K. M., and Dawson, J. H. (1993) *Inorg. Chem. 32*, 1460−1466.
36. Rublitz, C. (1977) *Biochem. Med. 17*, 13−19.
37. Ayling, J., Pirson, R., Pirson, W., and Boehm, G. (1973) *Anal. Biochem. 51*, 80−90.

38. Dawson, J. H., and Sono, M. (1987) *Chem. Rev. 87*, 1255−1276.
39. Scheele, J. S., Kharitonov, V. G., Martásek, P., Roman, L. J., Sharma, V. S., Masters, B. S. S., and Magde, D. (1997) *J. Biol. Chem. 272*, 12523−12528.
40. Mims, M. P., Porras, A. G., Olson, J. S., Noble, R. W., and Peterson, J. A. (1983) *J. Biol. Chem. 258*, 14219−14232.
41. Makino, R., Iizuka, T., Sakaguchi, K., and Ishimura, Y. (1982) in *Oxygenases and Oxygen Metabolism* (Nozaki, M., Yamamoto, S., Ishimura, Y., Coon, M. J., Ernster, L., and Estabrook, R. W., Eds.) pp 467−477, Academic Press.
42. Eisenstein, L., Debey, P., and Douzou, P. (1977) *Biochem. Biophys. Res. Commun. 77*, 1377−1383.
43. Presta, A., Siddhanta, U., Wu, C., Sennequier, N., Huang, L., Abu-Soud, H. M., Erzurum, S., and Stuehr, D. J. (1998) *Biochemistry 37*, 298−310.
44. Cleland, W. W. (1964) *Biochemistry 3*, 480−482.
45. Kaufman, S. (1959) *J. Biol. Chem. 234*, 2677−2682.
46. Olken, N. M., and Marletta, M. A. (1993) *Biochemistry 32*, 9677−9685.
47. Olken, N. M., Osawa, Y., and Marletta, M. A. (1994) *Biochemistry 33*, 14784−14791.
48. Salerno, J. C., McMillan, K., and Masters, B. S. S. (1996) *Biochemistry 35*, 11839−11845.
49. Migita, C. T., Salerno, J. C., Masters, B. S. S., Martásek, P., McMillan, K., and Ikeda-Saito, M. (1997) *Biochemistry 36*, 10987−10992.
50. Raman, C. S., Li, H., Martásek, P., Kral, V., Masters, B. S. S., and Poulos, T. L. (1998) *Cell 95*, 939−950.

BI990619H